EUROSTEEL 2005

4th European Conference on Steel and Composite Structures

Research – Eurocodes – Practice

Maastricht, The Netherlands
June 8-10, 2005

Organised by

Université de Liége, Belgium
Rheinisch-Westfälische Technische Hochschule Aachen, Germany
Technische Universiteit Eindhoven, The Netherlands

in co-operation with

ALMA, Maastricht

Edited by B. Hoffmeister and O. Hechler

Volume B

EXPERIMENTAL ANALYSIS ON STEEL AND LIGHTWEIGHT CONCRETE COMPOSITE BEAMS

Isabel Valente
Civil Engineering Department, University of Minho, Portugal
Departamento de Engª Civil, Universidade do Minho, Azurém, 4800-058 Guimarães, Portugal
Email: isabelv@civil.uminho.pt

Paulo J. S. Cruz
Civil Engineering Department, University of Minho, Portugal
Departamento de Engª Civil, Universidade do Minho, Azurém, 4800-058 Guimarães, Portugal
Email: pcruz@civil.uminho.pt

ABSTRACT

The present work describes the experimental tests on steel and lightweight concrete composite beams performed at University of Minho. The study involves tests on simply supported composite beams of 4.5 m span, with the same geometrical disposition, supports and materials. The geometrical configuration for the cross section and supports is identical for every beam, varying the shear connectors' distribution and the loading conditions. Headed studs are used to provide the connection between the steel profile and the concrete slab.

The parameters in study are the stud disposition and the load distribution. The main objective is to describe the composite beams behaviour, focused on its connection, and to analyse the contribution of the different components to the beams load and deformation capacity. All the tests explored the beams maximum load and deformation capacity and different types of failure were observed.

1 INTRODUCTION

The use of steel and concrete composite structures accounts for the contribution of the two materials, provided that a composite action exists between concrete and steel members. A composite action can be obtained, reducing or preventing the relative displacement of concrete and steel sections at their interface. Shear connectors are used to provide this composite action. Recent investigation proved that the use of shear studs is adequate when using high strength concrete [1]. Good results were also obtained with high strength lightweight concrete in "Push-out" tests recently performed [2] [3].

This communication describes the experimental tests on six simply supported steel and lightweight concrete composite beams with a 4.5 m span. The transversal section, span length and supporting conditions are identical for every beam. Shear connection elements distribution and load distribution are the varying parameters. Studs are used for shear connection and thus providing the composite action. The beams design puts particular emphasis on steel and lightweight concrete shear connection behaviour. In addition, the contribution of the different elements that constitute the beams on load and deformation capacity is analysed.

2 BEAMS IN STUDY

The beam is composed by an IPE120 steel profile and a 350 mm × 60 mm lightweight concrete slab (Fig. 1). Shear connection is provided with equally spaced shear studs of 13 mm diameter and 50 mm high. The shear connectors distribution is of three types: (1) total connection (8 studs ϕ13, h=50mm, in half span of the beam); (2) total connection associating connectors in pairs aiming a more ductile behaviour of the connection (8 studs ϕ13, h=50mm, in half span of the beam) [1]; and (3) partial connection (4 studs ϕ13, h=50mm, in half span of the beam) (Table 1).

Table 1 : Stud connectors distribution

Beam	Connection	Stud distribution	Loading
VM4	Total	Type 1	Loading 1
VM5	Total	Type 2	Loading 1
VM6	Partial	Type 3	Loading 1
VM7	Total	Type 1	Loading 2
VM3	Total	Type 2	Loading 2
VM8	Partial	Type 3	Loading 2

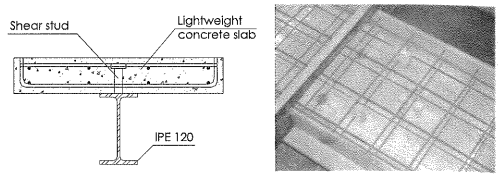

Fig. 1 : Transversal section and formwork

Two load configurations were considered (Fig. 2). The first corresponds to four concentrated loads, equally spaced of 900 mm along the beam, approximating a uniformly distributed loading. The second case corresponds to two concentrated loads closely spaced, near the beam mid span, approximating a concentrated loading. The corresponding bending moment and shear force diagrams are also presented in Fig. 2.

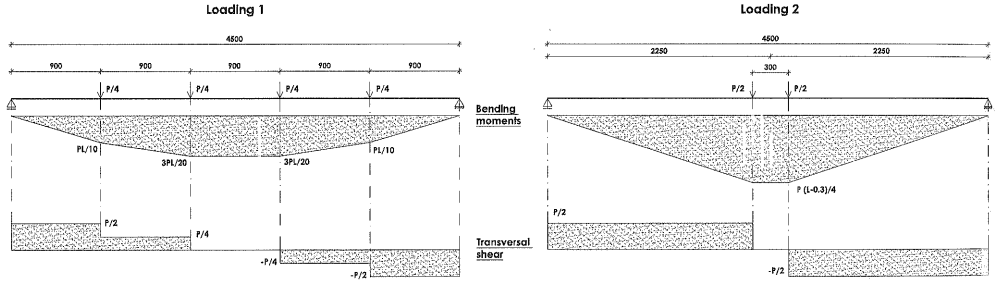

Fig. 2 : Loading and corresponding bending moment and shear force diagrams

The values for the materials tested are presented in Table 2. The medium values presented for each property are the average result of three specimens tests (Fig. 3).

Table 2 : Materials properties

Material Ref.	Beam	f_{cm} (MPa)	E_{cm} (GPa)	f_{ym} (MPa)	f_{um} (MPa)
BL33	VM4	55.60	22.08	-	-
BL32	VM5	64.40	25.00	-	-
BL34	VM6	54.72	23.82	-	-
BL38	VM7	58.36	22.00	-	-
BL37	VM3	60.49	22.02	-	-
BL39	VM8	58.16	22.23	-	-
Steel profile	All	-	-	335.7	491.1

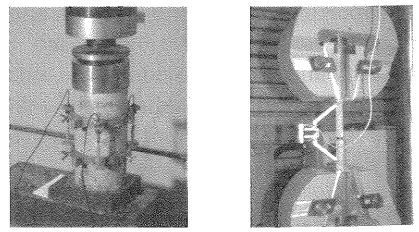

Fig. 3 : Materials testing

3 TEST SET UP

As represented in Fig. 4, the actuator load is divided into several smaller loads to put in place the different loading configurations. The set up is represented in Fig. 4 as well as the final test configuration, immediately before the test begins.

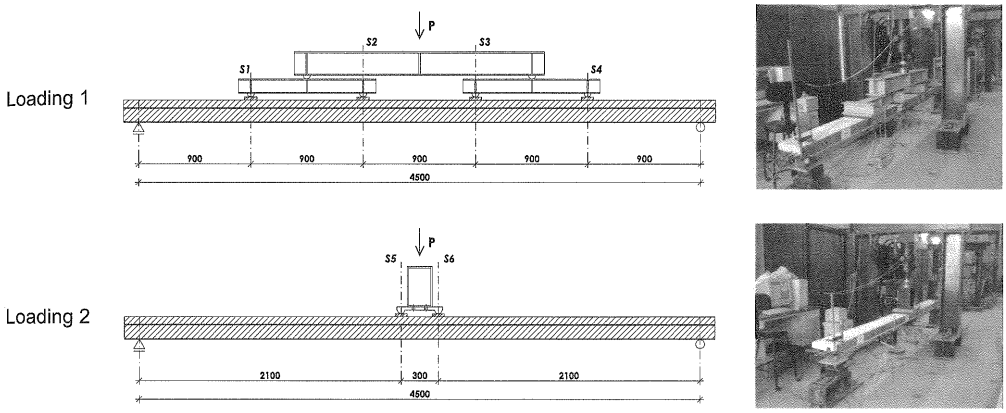

Fig. 4 : Test setup

The tests lead all the specimens to failure, and different types of collapse are observed. All tests are carried out with deformation control at the beam mid span and measurements of applied load value, vertical deformation along the beam, slip between steel profile and concrete slab and vertical separation between these two elements. Strain gauges are positioned in representative transversal sections in order to measure strain and curvature variation during the tests.

In order to establish critical sections for the beams, reference sections S1 to S6 are defined in Fig. 4. Sections A-A', B-B' e C-C' from Fig. 5 correspond to strain gauge localizations. Displacement transducers V1 to V3 measure the beam vertical deformation and displacement transducers H1 and H2 measure slip between the steel beam and the lightweight concrete slab. All of these measuring devices are represented in Fig. 5.

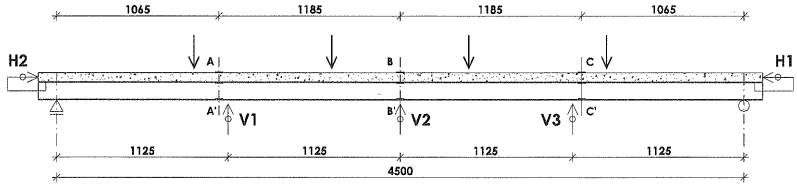

Fig. 5 : Monitoring and test control

4 RESULTS FROM TESTS

4.1 Failure modes

Beam VM4 shows a bending failure. Concrete crushes near the load application point at section S3. At the same time, concrete crushing initiates in the upper fibre near position S2. This occurs while a longitudinal crack at the concrete section mid height grows towards the

beam mid span (Fig. 6). Beam VM5 also shows a bending failure. Concrete crushes near the load point application at section S2. At the same time, concrete crushing initiates in the upper fibre, near position S3. VM5 failure is very similar to VM4 failure. Different from the previous beams, VM6 has a shear connection failure between the concrete slab and the steel beam. Connector failures are phased, with load capacity losses associated. This failure happens essentially in one side of the beam and vertical separation between steel beam and concrete slab is visible near the beam supports (Fig. 7).

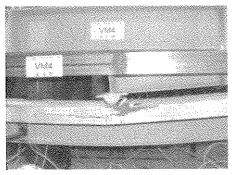

Fig. 6 : VM4 failure

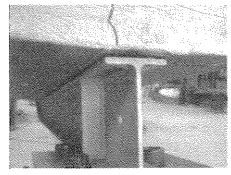

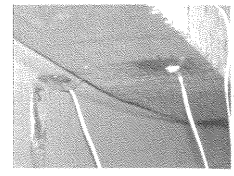

Fig. 7 : VM6 failure

Beam VM7 suffers a bending failure. Concrete crushes near the load point application at section S5, with a longitudinal crack at the concrete section mid height, growing towards the beam mid span (Fig. 8). The slab reinforcement near the crushing zone shows some local buckling (Fig. 8). Beam VM3 also shows a bending failure. Concrete crushes near the load point application at section S5, with a longitudinal crack at the concrete section mid height, growing towards the nearest support (Fig. 9).

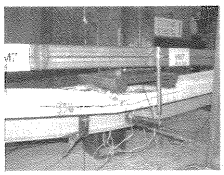

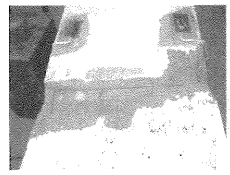

Fig. 8 : VM7 failure

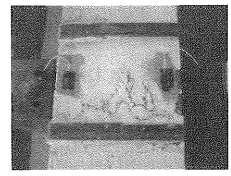

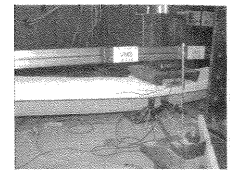

Fig. 9 : VM3 failure

VM8 suffers bending failure associated with shear connection failure (Fig. 10). Concrete crushing takes place at the upper fibre of both sections S5 and S6. At the final stages of loading, stud failure takes place in association with load capacity loss.

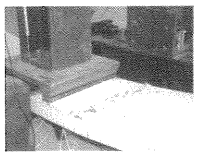

Fig. 10 : VM8 failure

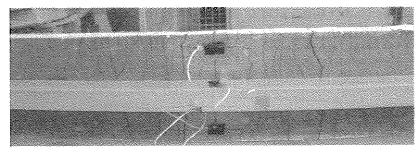

Fig. 11 : Distributed cracking

Fig. 12 : Slip

In all tested beams tensile cracks appear closely and similarly spaced at the bottom face of the concrete slab, along the failure zone (Fig. 11). Horizontal slip between steel profile and concrete slab is always visible (Fig. 12).

4.2 Load and deformation capacity

Load and corresponding bending moment failure values can be predicted through a limit state analysis. According to EC4 [4], bending failure is considered for beams with total connection design and the total plastic behaviour of the transversal section at failure is accepted, if it is classified as class 1. In the case of partial connection beam design, shear connection failure is admitted, resulting in an inferior value for the maximum bending moment.

In Table 3, predicted values for maximum sagging bending moment are presented ($M^{+}_{pl,R}$), in accordance with the materials properties previously determined. The values were determined considering always the maximum strain of 3.5 mm/m on the concrete slab. The stud failure is calculated according to equation (1), considering the value of 500 MPa for the steel ultimate tensile strength.

$$P_R = 0.8 f_u (\pi d^2/4) \quad (1)$$

Table 3 : Predicted maximum bending moments

Concrete Ref.	Beam	F_{cf} [kN]	F_{af} [kN]	Neutral axis position	x [m]	$M^{+}_{pl.R}$ [kN.m]	ε_y [mm/m]
BL33	VM4	992.46	443.46	Concrete slab	0.0268	47.27	20.00
BL32	VM5	1149.54		Concrete slab	0.0231	48.08	23.72
BL34	VM6	976.75		Concrete slab and steel flange	-	37.20	31.15
BL38	VM7	1041.73		Concrete slab	0.0255	47.55	21.17
BL37	VM3	1079.75		Concrete slab	0.0246	47.75	22.07
BL39	VM8	1038.16		Concrete slab and steel flange	-	37.43	32.69

F_{cf} – maximum compressive force to be mobilized at the concrete section ($F_{cf} = 0.85 \times f_{cm} \times A_c$)
F_{af} – maximum tensile force to be mobilized at the steel section ($F_{af} = f_{ym} \times A_a$)

Fig. 13 presents the experimental bending moment vs. vertical deformation diagram, measured at the beam mid span. All the beams show an initial elastic behaviour, approximate to estimated by an elastic approach, considering a total shear connection. Considering the elastic zone for both types of loading, the total connection hypothesis (VM4 and VM7) show higher stiffness, followed by the total connection and studs grouped in pairs hypothesis (VM5 and VM3) and the partial connection hypothesis (VM6 and VM8) comes at last, with a lower stiffness. A loss of stiffness is verified at each specimen for values over 0.45 M_{max}.

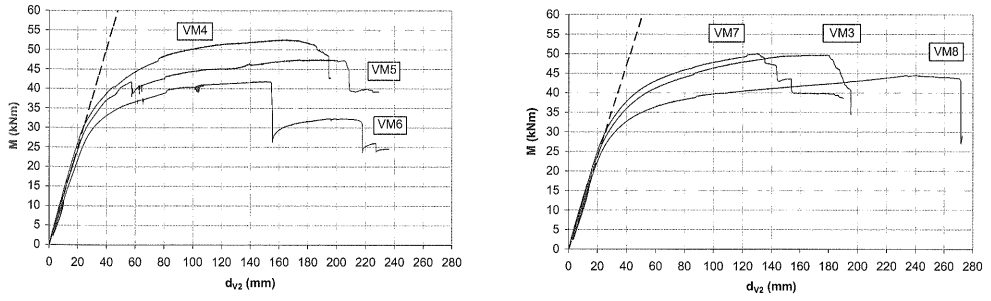

Fig. 13 : Maximum bending moment vs. vertical deformation (at beam mid span)

For the Loading 1 group, the beam vertical deformation correspondent to the maximum measured bending moment is similar for each type of total connection disposition, in spite of the different levels of loading. For the Loading 2 group, the maximum bending moment is very similar for both total connection beams, but the corresponding maximum vertical deformation is higher for VM3.

Before failure, VM6 and VM8 always present higher vertical deformation than the other beams, when comparing the same level of loading. Table 4 presents the experimentally determined values for bending moment and correspondent deformation.

The comparison of Table 3 and Table 4 puts in evidence some differences between measured and predicted bending moment values. Measured values are always higher than the predicted values (with the exception of VM5). The difference can result from steel tensile strength, as

higher values than the yield tensile strength can be attained in the steel section. Another possibility is a small deviation in the concrete slab dimensions, despite the efforts to make every slab similar, as was in general confirmed.

Table 4 : Maximum bending moment and corresponding beam vertical deformation (mid span)

Concrete Ref.	Beam	Test date	Failure type	M_{max} [kNm]	ε_y [mm/m]	ε_c [mm/m]	x [m]	$d\ (M_{max})$ [mm]
BL33	VM4	06-02-04	Bending	52.60	8.46	-3.12	0.0412	161.5 to 170.1
BL32	VM5	18-02-04	Bending	47.52	8.71	-2.67	0.0407	172.9 to 195.4
BL34	VM6	10-02-04	Shear connection	41.96	10.48	-1.94	-	146.6 to 154.3
BL38	VM7	05-04-04	Bending	50.10	15.64	-3.79	0.0383	124.2 to 130.9
BL37	VM3	13-04-04	Bending	49.76	15.62	-4.82	0.0437	157.1 to 180.4
BL39	VM8	16-04-04	Bend. & shear con.	44.51	*	-4.59	-	236.1 to 244.9

* - due to strain gauge ruin, these values were not measured
ε_y – value of strain measured at the lower fibber of the steel section
ε_c – value of strain measured at the upper fibber of the concrete section
x – measured from the concrete top layer

In every tested beam, the strain values in the steel section are lower than predicted. For total connection design beams, failure is conditioned by concrete, which means that the neutral axis position is lower than what was predicted, an aspect confirmed during the experimental testing, as showed in Table 4. It also means that in order to guarantee internal equilibrium, higher forces need to be mobilized in the steel section, overcoming the steel yield strength.

Higher values of strain at the steel lower fibre are attained for Loading 2 group, but not higher values for maximum bending moment. At the same time, the neutral axis position is close to the position measured for Loading 1 group, which means that the materials attain higher plastic strains and the increase of curvature and deflection result from these higher values.

For partial connection design beams, the difference between measured and predicted maximum bending moments can result from underestimating the value of the stud shear failure when using equation (1), as was shown in several "Push-out" tests, [1], and underestimating the studs flexibility, as it results in a decrease of shear stress flow through steel and concrete interface, retarding failure because of the redistribution of stress.

Fig. 14 and Fig. 15 illustrates the strain diagrams at the beam mid span section, for the maximum measured bending moment and for 40 % and 90 % of this value. For the lowest level of loading, $0.4M_{max}$, the strain distribution is uniform, with total compatibility between both materials. The steel to concrete connection guarantees the shear force transmission at this moment, even for beams with partial connection design.

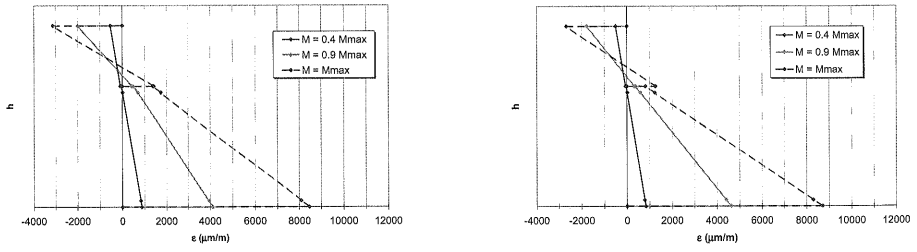

Fig. 14 : Strain diagram for VM4 (left) and VM5 (right)

The total interaction hypothesis is valid for VM4 even for maximum bending moment. An influence of the stud flexibility is observable for the other beams with total connection design,

like VM5, VM3 and VM7. In the case of VM5, total interaction is valid for most of the loading process, and the connection flexibility influence is only observable near the beam's failure. In both cases, the strain diagrams are very similar. A similar strain diagram for these two beams means that the vertical deformation (for maximum bending moment) is also approximate, as confirmed in Fig. 13. The fact that maximum bending moment for VM4 and VM5 is different reflects the worse connection efficiency of VM5, that results from a less efficient capacity to redistribute the stress between the elements, either concrete or steel, when one of them reaches its limit capacity. For VM6, the partial connection design results in a different strain diagram, where the connection's flexibility is visible from lower loads.

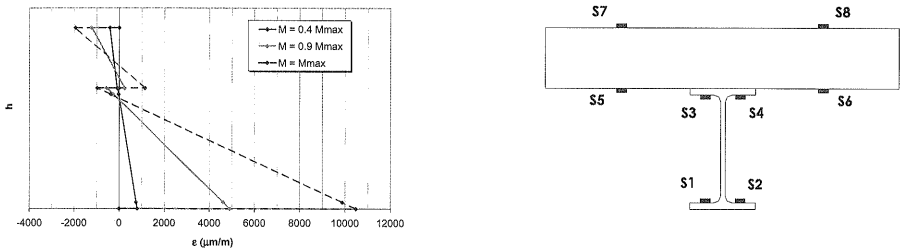

Fig. 15 : Strain diagram for VM6 (left) and strain gauges disposition (right)

In the initial phase of loading, the concrete slab is completely compressed, in every tested beam. With the loading increase, the neutral axis goes up and tensile stress begins at the concrete slab lower fibbers. This change comes for values of 37.1 kNm and 36.2 kNm for VM4 and VM5, respectively. For beam VM6, tensile stress at the concrete slab begin earlier, for 32.5 kNm, with significant values of slip registered for this level of loading.

Fig. 16 shows the slip values for VM4 and VM6. On beam VM4, initially both transducers measure similar values of slip. On the final phase of the test, H1 measures values that are a bit higher than H2 and failure initiates at section S3, positioned on the same half side of the beam. The values measured for VM6 are much higher than the ones for VM4, and grows particularly on one side of the beam (measured by H2). In the test initial phase, the slip evolution measured by both transducers is very similar. Following the failure of the first connector, the slip growth concentrates on one side of the beam ending with the progressive failure of all the studs localized at this half.

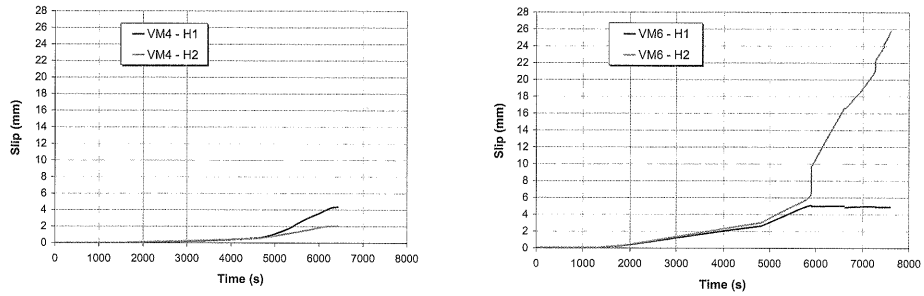

Fig. 16 : Horizontal slip for beams VM4 (left) and VM6 (right)

On beam VM3, initially both transducers measure similar values of slip (Fig. 17). On the final phase of the test, H2 measures values that are a bit higher than H1 and failure initiates at section S5, positioned on the same half side of the beam. In beam VM8, the horizontal slip tends to be higher when compared to the other beams of the same loading group. The

connectors' failures occur in H2 half side of the beam, coincidently with the bending failure localized at section S5 and S6.

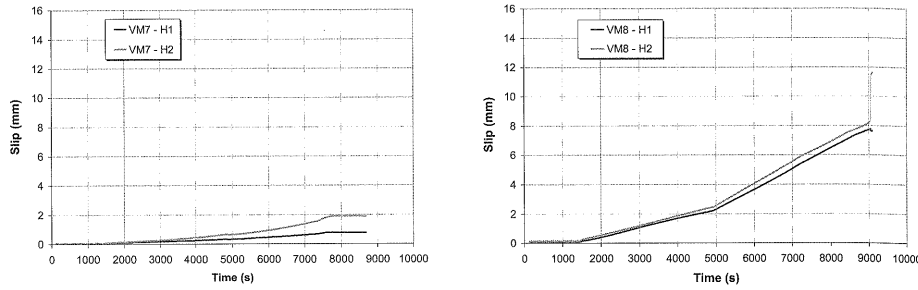

Fig. 17 : Horizontal slip for beams VM3 (left) and VM8 (right)

In general, the values of slip measured for the Loading group 1 are higher than the values measures for the Loading group 2, which is expected, since the total applied load value is higher.

5 SUMMARY

This work, made it possible to analyse the behaviour of steel and lightweight concrete composite beams. In a global level, a good behaviour is observed, similar to what could be expected for normal density concrete. The steel to concrete connection shows good behaviour, as shear connection failure always occurs, instead of concrete smashing near the stud position. The uniform and equally spaced stud distribution is the most efficient type of connection, allowing the higher load capacity. Grouping studs in pairs allowed larger vertical deformation but resulted in a reduction of the load capacity.

ACKNOWLEDGMENTS

The present work was financed by the Investigation Project *Sapiens* ECM/33067/99 - "*Steel-concrete composite bridges*: *Use of lightweight high performance concrete*", from Program PRAXIS XXI. We also thank the Structural Civil Engineering Laboratory at University of Minho, where the tests were performed.

6 REFERENCES

[1] Hegger, J. et al: *Studies on the ductility of shear connectors when using high-strength concrete*; Int. Symp. on Connections between Steel and concrete, Vol.2, pp 1025-1045, University of Stuttgart, 10-12 Setembro 2001.

[2] Valente, I., Cruz, P. J. S.: *"Caracterização da ductilidade de ligações aço-betão leve com conectores tipo perno"*, 4º Congresso de Construção Metálica e Mista, 4 e 5 de Dezembro de 2003, Lisboa, IST, Portugal.

[3] Cruz, P. J. S.; Valente, I.; Hegger, J.; Rauscher, S.; Goralski, C.: *"Experimental studies on shear connection between steel and lightweight concrete using studs"*, Eurosteel 2005, Maastricht, The Netherlands.

[4] Eurocode 4, ENV 1994: *Design of composite steel and concrete structures*, CEN, 1994.

KEYWORDS

Composite beams, lightweight concrete; shear connection; experimental testing; slip.